Crystal Structure, Solution Chemistry, and Antitumor Activity of Diastereomeric [1,2-Bis(2-hydroxyphenyl)ethylenediamine]dichloroplatinum(II) Complexes

Ronald Gust,*,† Helmut Schönenberger,† Jürgen Kritzenberger,‡ Klaus-Jürgen Range,§ Ulrich Klement,§ and Thomas Burgemeister‖

Institut für Pharmazie, Institut für Physikalische Chemie, Institut für Anorganische Chemie, and Institut für Organische Chemie, Universität Regensburg, Universitätsstrasse 31, 93040 Regensburg, Germany

Received September 30, 1992®

Complete three-dimensional X-ray crystal structure analyses of *meso*- and *S,S*-configurated [1,2-bis(2-hydroxyphenyl)-ethylenediamine]dichloroplatinum(II) complexes (*meso*-**3**-$PtCl_2$ and (–)-**3**-$PtCl_2$) have been carried out. Data were collected at room temperature. After anisotropic refinement of *F*-values by least squares, *R* is 0.098 for the *meso*-configurated complex and 0.048 for the *S,S*-configurated complex. *meso*- and (–)-**3**-$PtCl_2$ crystallize with 4 molecules in a unit cell of monoclinic symmetry. The space group is $P2_1/n$ for *meso*-**3**-$PtCl_2$ with cell dimensions a = 11.032 Å, b = 11.671 Å, c = 12.347 Å, and β = 111.17° and $P2_1$ for (–)-**3**-$PtCl_2$ with a = 9.969 Å, b = 11.263 Å, c = 14.560 Å, and β = 107.73°. *meso*-**3**-$PtCl_2$ and (–)-**3**-$PtCl_2$, respectively, build dimeric units. The ethylenediamine ligand of *meso*-**3**-$PtCl_2$ is puckered and exists in an envelope conformation, while the molecules of the dimeric units of (–)-**3**-$PtCl_2$ show both the envelope and the half-chair conformation. Both aromatic rings of (–)-**3**-$PtCl_2$ are equatorially arranged and fixed by intramolecular hydrogen bonds from the amino protons to the phenolic oxygen. The hydroxy group of the axially standing ring of *meso*-**3**-$PtCl_2$ is not involved in intramolecular N–H···O bridges since it is oriented opposite to the NH_2 groups. In solution, however, this OH group is reoriented and builds H–H···O bonds, too. The influence of the 3D structure on the reactivity of the complexes was investigated through the substitution of the Cl^- leaving groups by I^-. The substitution follows an associative mechanism, whereby the rate constants are given by the equation $k_{obs} = k_s + k_{I^-}[I^-]$ in accordance with the possible reaction pathways. K_s is the rate constant for the I^- coordination after hydrolysis and k_{I^-} the rate constant for the direct nucleophilic attack. Due to the shielding of the platinum by the axially oriented aromatic ring, the reactivity of *meso*-**3**-$PtCl_2$ ($k_{1,s}$ = 3.06 × 10^{-5} s^{-1}, k_{1,I^-} = 383.5 L/mol·s, $k_{2,s}$ = 1.26 × 10^{-5} s^{-1}, k_{2,I^-} = 120.2 L/mol·s) is decreased compared to (–)-**3**-$PtCl_2$ ($k_{1,s}$ = 5.05 × 10^{-5} s^{-1}, k_{1,I^-} = 543.9 L/mol·s, $k_{2,s}$ = 1.64 × 10^{-5} s^{-1}, k_{2,I^-} = 191.6 L/mol·s). The reactivities correlate very well with the antitumor results *in vivo* on the P388 leukemia of the mouse and *in vitro* for the NIH-OVCAR 3 cell line. In accordance with the high reactivity the best antitumor effects were found for (–)-**3**-$PtCl_2$. For the P388 leukemia of the mouse a dose of 6.6 μmol/kg given on days 1–5 leads to survival of all the animals at the end of the test.

Introduction

Since the discovery of the antitumor activity of *cis*-diamminedichloroplatinum(II)[1,2] (cisplatin, DDP; for formula see Chart I) in 1965, extensive research has been done to establish the mechanism of antitumor action and toxicity of platinum complexes.

Nowadays it is generally accepted that the cytotoxic effects of platinum complexes result from the binding to DNA. After the first and rate-determining hydrolysis step, the formed aquachloroplatinum(II) complex coordinates preferentially to guanine bases of the DNA.[3] Subsequent reaction with an adjacent nucleobase leads to a damage of the DNA.

On the other hand, it has been suggested that the reaction with other bionucleophiles, especially S-containing nucleophiles, proceeds by a direct nucleophilic substitution of the chloride ligand without prior formation of the aquachloroplatinum(II) species.[4]

Chart I

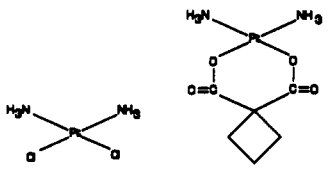

Cisplatin Carboplatin

Compd.	Config.
meso-3-$PtCl_2$	R,S
(+)-3-$PtCl_2$	R,R
(–)-3-$PtCl_2$	S,S

Since this kind of reaction is of great importance for the inactivation of the drug in the course of the transport to the tumor and for toxic side effects, the reactive Cl^- leaving groups were exchanged by more stably bonded leaving groups, like cyclobutane-1,1-dicarboxylate,[5] which are inert for a direct nucleophilic substitution.

The diammine(cyclobutane-1,1-dicarboxylato)platinum(II) complex (carboplatin; for formula see Chart I) indeed possesses reduced toxicity but also lower antitumor activity, due to its low hydrolysis rate.[6] Therefore many groups tried to reduce the side

† Institut für Pharmazie.
‡ Institut für Physikalische Chemie.
§ Institut für Anorganische Chemie.
‖ Institut für Organische Chemie.
• Abstract published in *Advance ACS Abstracts,* October 1, 1993.

(1) Rosenberg, B.; Van Camp, L.; Krigas, T. *Nature* (*London*) **1965**, *205*, 698.
(2) Rosenberg, B. *Biochimie* **1978**, *60*, 859.
(3) Johnson, N. P.; Hoeschele, J. D.; Rahn, R. O. *Chem. Biol. Interact.* **1980**, *30*, 151.
(4) Repta, A. J.; Long, D. F. In *Cisplatin Current Status and New Developments*; Prestayko, A. W., Crooke, S. T., Carter, S. K., Eds.; Academic Press: New York, 1980; p 285.
(5) Cleare, M. J.; Hydes, B. W.; Malerbi, B. W.; Watkins, D. M. *Biochimie* **1978** *60*, 835 and references therein.

0020-1669/93/1332-5939$04.00/0

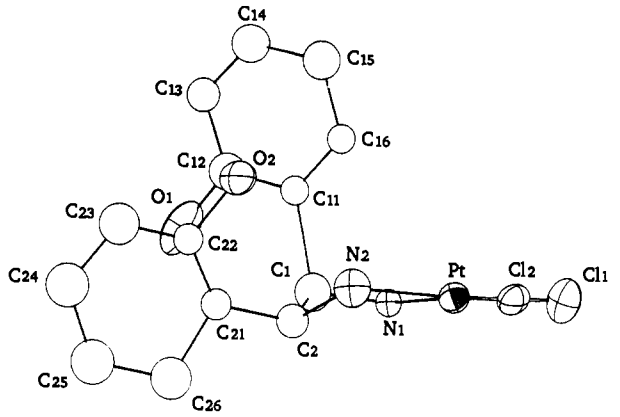

Figure 1. ORTEP plot, showing the *meso*-3-$PtCl_2$ molecule.

effects of cisplatin by variation of the neutral ligand. Among the great number of complexes synthesized in the last 10 years, complexes bearing the 1,2-diphenylethylenediamine ligand were found to be potent antitumor agents. Dependent on the substituents in the aromatic rings, the complexes give rise to selective effects on various tumors and proved to be less toxic and more potent than cisplatin.[7-10] The complexes with the highest antitumor potency of this series are the enantiomeric [1,2-bis-(2-hydroxyphenyl)ethylenediamine]dichloroplatinum(II) complexes (–)-3-$PtCl_2$ and (+)-3-$PtCl_2$ (for formula see Chart I). *In vitro* on the NIH:OVCAR-3 cell line they reduced the cell growth more strongly than cisplatin. Interestingly their diastereomer *meso*-3-$PtCl_2$ (for formula see Chart I) is significantly less active.

To understand the reason for these different tumor-inhibiting effects we investigated the influence of the ligand configuration and conformation on the reactivity and the antitumor activity of the diastereomeric complexes *meso*-3-$PtCl_2$ and (–)-3-$PtCl_2$.

In this paper we describe the spatial structure of (–)-3-$PtCl_2$ and *meso*-3-$PtCl_2$ in the solid state and in solution as well as their solution chemistry. We used the reaction of the complexes with I^- as a nucleophilic agent to estimate the influence of the 1,2-diphenylethylenediamine ligand on the nucleophilic substitution of the platinum(II) complexes. The reactivity will be correlated with the *in vitro* effects on the NIH:OVCAR-3 cell line and the *in vivo* activity and toxicity obtained from the test on the murine lymphocytic leukemia P388.

Results and Discussion

X-ray Structure Analysis. The atomic positional parameters of *meso*-3-$PtCl_2$ and (–)-3-$PtCl_2$ are listed in Tables II and III. Tables IV and V present important bond lengths and angles. For the numbering of the atoms see Figures 1 and 3.

meso-3-$PtCl_2$ crystallizes with four molecules in the unit cell of space group $P2_1/n$ (see Table I). Two molecules, linked over an inversion center, build a symmetric dimeric unit, separated by a Pt···Pt distance of 3.419 Å. Stabilization of the dimers is mediated by interaction of the platinum orbitals and reciprocal H-bridges between the amino protons and the Cl^- leaving groups of the two molecules of a dimeric unit. Prerequisite for this is a distance between the molecules shorter than 3.5 Å.[11] Between dimeric units strong interactions can be excluded, due to the Pt···Pt distance of 7.642 Å and the slight lateral deviation from the ideal Pt···Pt stacking along the crystallographic *c*-axis. The arrangement of the dimeric units of *meso*-3-$PtCl_2$ is shown in Figure 2.

(–)-3-$PtCl_2$ shows a similar arrangement of the molecules. It crystallizes with four molecules in the unit cell with space group $P2_1$ (see Table I). The dimeric units, however, consist of two

Table I. Experimental Data for the X-ray Diffraction Study

	meso-3-$PtCl_2$	(–)-3-$PtCl_2$
formula	$C_{14}H_{16}N_2Cl_2O_2Pt$	$C_{14}H_{16}N_2Cl_2O_2Pt$
fw	510.29	510.29
cryst system	monoclinic	
space group	$P2_1/n$	$P2_1$
data collecn temp, °C	25	23
radiation (λ, Å)	Mo, graphite (0.710 73)	
a, Å	11.032(9)	9.969(2)
b, Å	11.671(9)	11.263(2)
c, Å	12.347(14)	14.560(2)
β, deg	111.17(8)	107.73(1)
V, Å^3	1482(2)	1557.2
Z	4	4
D_{calc}, g·cm^{-1}	2.29	2.18
F(000)	968	968
cryst dimens, μm	45 × 60 × 150	15 × 60 × 120
linear abs coeff, mm^{-1}	993	946
max–min transm factors	0.72–1.0	0.66–1.0
diffractometer	Enraf-Nonius CAD4	
scan type	χ/2θ	
max time per reflcn, s	60	
scan width, deg	0.8 + 0.35 tan θ	0.7 + 0.35 tan θ
θ range, deg	2–25	2–27.5
no. of reflcns, measd	5180	6498
no. of unique data	3184	4867
no. of unique obsd data [$I > 1\sigma(I)$]	1558	2286
variables	110	218
R	0.098	0.048
R_w	0.119	0.035
R_{int}	0.047	0.037
w	$4I/\sigma^2(I)$	

Table II. Positional Parameters[a] and Equivalent Isotropic Displacement Parameters (Å^2) of *meso*-3-$PtCl_2$

atom	*x*	*y*	*z*	B^b
Pt	0.6483(1)	0.0082(1)	0.4862(1)	2.35(2)
Cl_1	0.7035(8)	0.1589(9)	0.6147(7)	3.9(2)
Cl_2	0.5552(7)	0.1282(8)	0.3275(6)	2.9(2)
O_1	0.855(2)	–0.436(3)	0.624(2)	5.4(7)
O_2	0.759(2)	–0.292(2)	0.308(2)	3.5(5)
N_1	0.718(2)	–0.117(2)	0.621(2)	1.8(4)[c]
N_2	0.618(2)	–0.133(3)	0.387(2)	3.6(6)[c]
C_1	0.713(3)	–0.226(3)	0.569(3)	3.5(7)[c]
C_2	0.614(3)	–0.242(3)	0.464(2)	2.7(6)[c]
C_{11}	0.870(2)	–0.248(3)	0.560(2)	2.1(6)[c]
C_{12}	0.919(3)	–0.356(3)	0.585(3)	3.4(7)[c]
C_{13}	1.042(3)	–0.389(3)	0.584(2)	2.9(6)[c]
C_{14}	1.104(3)	–0.308(4)	0.552(3)	3.7(8)[c]
C_{15}	1.051(3)	–0.192(4)	0.515(3)	3.8(8)[c]
C_{16}	0.926(2)	–0.166(3)	0.521(2)	2.1(6)[c]
C_{21}	0.605(3)	–0.346(3)	0.387(2)	2.4(6)[c]
C_{22}	0.676(2)	–0.375(3)	0.325(2)	2.3(6)[c]
C_{23}	0.673(3)	–0.471(4)	0.264(4)	4.2(8)[c]
C_{24}	0.584(3)	–0.555(4)	0.269(3)	4.8(9)[c]
C_{25}	0.497(3)	–0.532(4)	0.336(3)	4.9(9)[c]
C_{26}	0.499(3)	–0.422(4)	0.400(3)	4.4(8)[c]

[a] Esds in the least significant digits are shown in parentheses. [b] Anisotropically refined atoms are given in form of the isotropic equivalent displacement parameter defined as $^4/_3[a^2B(1,1) + b^2B(2,2) + c^2B(3,3) + ab(\cos\gamma)B(1,2) + ac(\cos\beta)B(1,3) + bc(\cos\alpha)B(2,3)]$. [c] Isotropically refined.

(6) Schurig, J. E.; Rose, W. C.; Catino, J. J.; Gaver, R. C.; Long, B. H.; Madissoo, H.; Canetta, R. In *Carboplatin* (JM8). Current perspectives and future directions; Brunn, P. A., Jr., Canetta, R., Ozols, R. F., Rozencweig, M., Eds.; W. B. Saunders Co.: Philadelphia, PA, 1990; p 3.
(7) Jennerwein, M.; Wappes, B.; Gust, R.; Schönenberger, H.; Engel, J.; Seeber, S.; Osieka, R. *J. Cancer Res. Clin. Oncol.* **1988**, *114*, 347.
(8) Gust, R.; Schönenberger, H. *Eur. J. Med. Chem.* **1993**, *28*, 103–115.
(9) Karl, J.; Gust, R.; Spruss, Th.; Schneider, M. R.; Schönenberger, H.; Engel, J.; Wrobel, K. H.; Lux, F.; Trebert-Haeberlin, S. *J. Med. Chem.* **1988**, *31*, 72.
(10) Müller, R.; Gust, R.; Bernhardt, G.; Keller, Chr.; Schönenberger, H.; Seeber, S.; Osieka, R.; Eastman, A.; Jennerwein, M. *J. Cancer Res. Clin. Oncol.* **1990**, *116*, 237.
(11) Milburn, G.; Truter, M. *J. Chem. Soc. A* 1966, 1609.

Table III. Positional Parameters[a] and Equivalent Isotropic Displacement Parameters (Å^2) of (–)-3-$PtCl_2$

	molecule 1					molecule 2			
atom	*x*	*y*	*z*	B^b	atom	*x*	*y*	*z*	B^b
Pt_1	0.86417(6)	0.773	0.70646(5)	2.38(1)	Pt_2	0.60824(6)	0.84022(8)	0.79828(5)	2.14(1)
Cl_{11}	0.9607(5)	0.6358(5)	0.8245(4)	4.0(1)	Cl_{21}	0.7410(5)	0.9797(5)	0.9065(3)	3.6(1)
Cl_{12}	0.7282(5)	0.6388(5)	0.6010(4)	3.9(1)	Cl_{22}	0.5173(5)	0.9921(5)	0.6896(4)	3.7(1)
O_{11}	1.227(1)	0.998(1)	0.7405(9)	3.4(3)	O_{21}	0.478(1)	0.558(1)	0.9759(8)	2.8(3)
O_{12}	1.033(1)	1.078(1)	0.4984(9)	3.9(4)	O_{22}	0.199(1)	0.590(1)	0.736(1)	4.5(4)
N_{11}	0.982(1)	0.907(1)	0.7940(9)	2.7(3)[c]	N_{21}	0.681(1)	0.707(1)	0.891(1)	2.5(3)[c]
N_{12}	0.792(1)	0.912(1)	0.6110(8)	1.8(3)[c]	N_{22}	0.487(1)	0.719(1)	0.7119(9)	2.3(3)[c]
C_{11}	0.947(2)	1.027(2)	0.745(1)	2.1(3)[c]	C_{21}	0.627(2)	0.587(2)	0.837(1)	1.9(3)[c]
C_{12}	0.910(2)	1.007(2)	0.639(1)	2.1(3)[c]	C_{22}	0.478(2)	0.615(2)	0.777(1)	2.1(3)[c]
C_{31}	1.059(2)	1.121(2)	0.784(1)	2.6(4)[c]	C_{51}	0.656(2)	0.487(2)	0.910(1)	2.0(3)[c]
C_{32}	1.194(2)	1.101(2)	0.782(1)	2.2(3)[c]	C_{52}	0.583(2)	0.479(2)	0.974(1)	2.7(4)[c]
C_{33}	1.314(2)	1.189(2)	0.832(1)	4.0(5)[c]	C_{53}	0.613(1)	0.381(1)	1.044(1)	2.0(3)[c]
C_{34}	1.264(2)	1.280(2)	0.870(1)	3.4(4)[c]	C_{54}	0.712(2)	0.307(1)	1.039(1)	2.5(4)[c]
C_{35}	1.126(2)	1.305(2)	0.868(1)	5.0(5)[c]	C_{55}	0.788(2)	0.312(2)	0.973(1)	2.7(4)[c]
C_{36}	1.027(2)	1.218(2)	0.832(1)	3.0(3)[c]	C_{56}	0.758(2)	0.412(2)	0.905(1)	3.8(5)[c]
C_{41}	0.861(2)	1.120(2)	0.581(1)	2.3(4)[c]	C_{61}	0.404(1)	0.511(1)	0.716(1)	1.1(3)[c]
C_{42}	0.924(2)	1.154(2)	0.510(1)	2.4(4)[c]	C_{62}	0.257(2)	0.496(2)	0.697(1)	2.8(4)[c]
C_{43}	0.890(2)	1.260(2)	0.459(1)	2.8(4)[c]	C_{63}	0.186(2)	0.400(2)	0.649(1)	3.5(4)[c]
C_{44}	0.789(2)	1.336(2)	0.471(1)	2.9(4)[c]	C_{64}	0.253(2)	0.313(2)	0.616(1)	2.7(4)[c]
C_{45}	0.722(2)	1.304(2)	0.541(1)	3.2(4)[c]	C_{65}	0.394(2)	0.325(2)	0.629(1)	2.9(4)[c]
C_{46}	0.755(2)	1.198(2)	0.591(1)	3.6(5)[c]	C_{66}	0.477(2)	0.420(2)	0.686(1)	3.4(4)[c]

[a–c] See Table II.

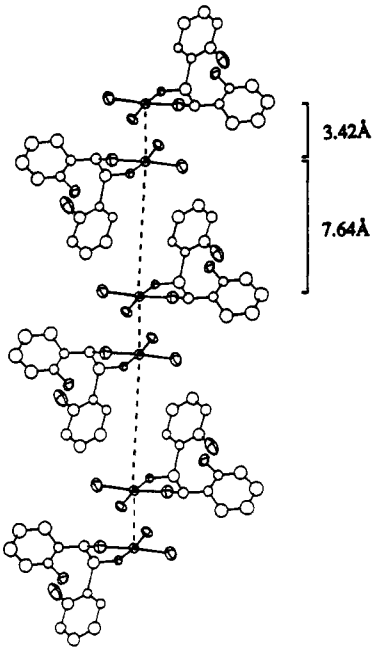

Figure 2. View of the stacking arrangement of *meso*-3-$PtCl_2$.

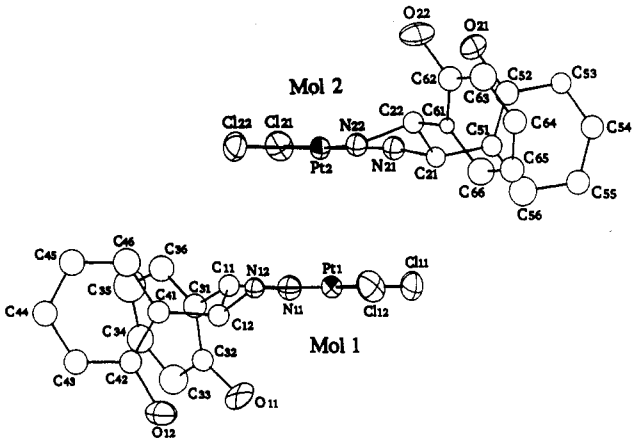

Figure 3. ORTEP plot, showing the two conformeric (–)-3-$PtCl_2$ molecules.

molecules (molecules 1 and 2) of different conformeric structure. The Pt···Pt separations between the paired molecules are 3.308 and 7.165 Å between two dimers (see Figure 4). The arrangement of the diastereomeric [1,2-bis(2-hydroxyphenyl)ethylenediamine]-dichloroplatinum(II) molecules in the crystals is different from that of cisplatin and dichloroethylenediamineplatinum(II) ($enPtCl_2$).

Cisplatin crystals are triclinic with two molecules in the unit cell. The square planar molecules build columnar structures with Pt···Pt separations of alternatively 3.409 and 3.372 Å.[11] Introduction of ethylenediamine as ligand does not effect a change of the structure, though the resulting five-membered chelate ring is strongly puckered (±0.43 Å out of the platinum plane). $enPtCl_2$ exists in isomorphous crystals of space group $C222_1$ and 4 molecules in the unit cell separated by Pt···Pt distances of 3.381 Å.[12]

By comparison of these data with those of *meso*-3-$PtCl_2$ and (–)-3-$PtCl_2$ a possible reason for the existence of [1,2-bis(2-hydroxyphenyl)ethylenediamine]dichloroplatinum(II) dimers in solid state is found in the aromatic rings. In both cases intermolecular repulsions of the bulky phenyl residues hinder the closer approach of the dimers and therefore the development of columnar structures. The aromatic rings in (–)-3-$PtCl_2$ are exclusively bis-equatorially arranged. The second possible conformeric form with rings standing bis-axially is not realized. On the other hand, in both conformeric forms of *meso*-3-$PtCl_2$ one ring is always equatorially and one ring axially oriented. The latter increases the repulsion compared to an equatorial one so the *meso*-3-$PtCl_2$ dimers have a distance to each other which is 0.48 Å larger than that of (–)-3-$PtCl_2$.

In contrast to $enPtCl_2$, which exists in a half-chair conformation, the second energetically favored structure, an envelope conformation, is realized in *meso*-3-$PtCl_2$ and in molecule 1 of (–)-3-$PtCl_2$. In *meso*-3-$PtCl_2$ the benzylic C_1-atom is twisted by 0.05 Å and the C_2-atom by 0.49 Å out of plane (see Figure 1). Molecule 1 of (–)-3-$PtCl_2$ exists in a puckering with C_{11} 0.072 Å above and C_{12} 0.643 Å under the N–Pt–N plane. Molecule 2 of the dimeric unit of (–)-3-$PtCl_2$ possesses a half-chair structure with C_{21} 0.239 Å above and C_{22} 0.547 Å below the plane (see Figure 3). The aromatic substituents in the 3-$PtCl_2$ stereoisomers also influence the spatial arrangement of the atoms neighboring the platinum.

Examinations on $enPtCl_2$ have shown that the N–Pt–N angle is reduced from nearly 90°, as found for cisplatin, to 73° in its

Table IV. Selected Bond Angles (deg) and Torsional Angles (deg)[a]

(−)-3-$PtCl_2$				*meso*-3-$PtCl_2$	
molecule 1		molecule 2			
N_{12}–Pt_1–N_{11}	83.04(13)	N_{22}–Pt_2–N_{21}	86.46(13)	N_2–Pt–N_1	81.24(12)
N_{12}–Pt_1–Cl_{12}	92.06(13)	N_{22}–Pt_2–Cl_{22}	92.14(12)	N_2–Pt–Cl_2	93.25(12)
N_{11}–Pt_1–Cl_{11}	90.08(13)	N_{21}–Pt_2–Cl_{21}	92.04(14)	N_1–Pt–Cl_1	93.29(12)
Cl_{12}–Pt_1–Cl_{11}	94.82(12)	Cl_{22}–Pt_2–Cl_{21}	89.29(12)	Cl_1–Pt–Cl_2	92.43(12)
N_{11}–C_{11}–C_{12}–N_{12}	54(2)	N_{21}–C_{21}–C_{22}–N_{22}	58(2)	N_1–C_1–C_2–N_2	49(4)
N_{12}–Pt_1–N_{11}–C_{11}	3(1)	N_{22}–Pt_2–N_{21}–C_{21}	10(1)	N_1–Pt–N_2–C_2	20(2)
N_{11}–C_{11}–C_{31}–C_{32}	57(2)	N_{21}–C_{21}–C_{51}–C_{52}	70(2)	N_1–C_1–C_{11}–C_{12}	139(2)
N_{12}–C_{12}–C_{41}–C_{42}	−111(2)	N_{22}–C_{22}–C_{61}–C_{62}	−93(2)	N_2–C_2–C_{21}–C_{22}	50(4)

[a] See Table II.

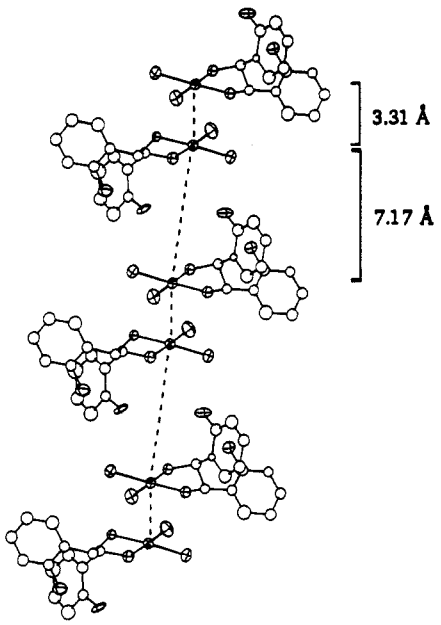

Figure 4. View of the stacking arrangement of (−)-3-$PtCl_2$.

puckered five-membered chelate ring.[12] The other angles are expanded to 95.3° (N–Pt–Cl) and 96.4° (Cl–Pt–Cl).

The bis-equatorially arranged phenyl rings in the half-chair conformation of (−)-3-$PtCl_2$ (molecule 2) increase the N–Pt–N angle to 86.46°, so the platinum environment is similar to that of cisplatin with Pt–N distances of Pt_2–N_{22} = 1.99 Å and Pt_2–N_{21} = 2.00 Å (cisplatin = 2.01 ± 0.04 Å) and Pt–Cl bonds of 2.32 and 2.34 Å (cisplatin: Pt–Cl = 2.33 Å).[11] The envelope structure of molecule 1 leads to a N–Pt–N angle of 83.04°, increased Pt–N bond lengths of 2.07 and 2.09 Å, and shorter Pt–Cl distances of 2.28 and 2.29 Å (see Table V).

In *meso*-3-$PtCl_2$, the aromatic rings are synclinally arranged with one equatorially and one axially standing ring. Due to the higher repulsion, a lower puckering of the envelope conformation and different Pt–N and Pt–Cl bond lengths are observed (Pt–N_2 = 2.01 Å; Pt–N_1 = 2.13 Å; Pt–Cl_1 = 2.295 Å; Pt–Cl_2 = 2.316 Å; see Table V). The equatorially arranged rings are fixed by hydrogen bonds from the amino protons to the oxygens of the phenolic residues.

In the molecules of (−)-3-$PtCl_2$ the rings are arranged with dihedral angles of 70° (molecule 1) and 41° (molecule 2) and the hydroxy groups are oriented toward the N–Pt–N plane. Therefore, hydrogen bonds can be formed due to an O–N distance smaller than 3.5 Å between O_{11}–N_{11} (2.96 Å) of molecule 1 as well as O_{21}–N_{21} (3.15 Å) and O_{22}–N_{22} (3.34 Å) of molecule 2 (see Table V). However, the orientation of the OH compared to the NH_2 group deviates from the ideal angle of −180°, e.g. N_{12}–C_{12}–C_{41}–C_{42} = −111° (see Table IV). It is assumed that after dissolution an optimal conformation for strong hydrogen bonds is formed. O–H···O hydrogen bonds between the hydroxy groups are not present in the solid state owing to the large O–O distance of 3.58 and 3.769 Å (see Table V).

(12) Iball, J.; MacDougall, M.; Scrimgeour, S. *Acta Crystallogr.* **1975**, *B31*, 1672.

Table V. Selected Bond Lengths (Å) and Distances (Å)[a]

(−)-3-$PtCl_2$				*meso*-3-$PtCl_2$	
molecule 1		molecule 2			
Pt_1–N_{11}	2.09(2)	Pt_2–N_{21}	2.00(2)	Pt_1–N_1	2.13(2)
Pt_1–N_{12}	2.07(2)	Pt_2–N_{22}	1.99(2)	Pt_1–N_2	2.01(3)
Pt_1–Cl_{11}	2.29(1)	Pt_2–Cl_{21}	2.34(1)	Pt_1–Cl_1	2.295(9)
Pt_1–Cl_{12}	2.284(9)	Pt_2–Cl_{22}	2.32(1)	Pt_2–Cl_2	2.316(8)
Pt_1–Pt_2	3.308(6)	Pt_2–Pt_3	7.165(6)	Pt_1–Pt_2	3.419(1)
				Pt_2–Pt_3	7.642(1)
O_{11}–N_{11}	2.96(1)	O_{21}–N_{21}	3.15(1)	O_1–N_1	4.01(4)
O_{11}–N_{12}	4.28(1)	O_{21}–N_{22}	4.28(2)	O_1–N_2	4.72(4)
O_{12}–N_{11}	4.87(2)	O_{22}–N_{21}	4.83(1)	O_2–N_1	4.54(3)
O_{12}–N_{12}	3.79(1)	O_{22}–N_{22}	3.34(1)	O_2–N_2	2.82(3)
O_{12}–O_{11}	3.58(2)	O_{21}–O_{22}	3.77(2)	O_2–O_1	4.01(3)
C_{11}–C_{12}	1.50(3)	C_{21}–C_{22}	1.51(3)	C_1–C_2	1.36(4)
C_{11}–N_{11}	1.51(3)	C_{21}–N_{21}	1.57(3)	C_1–N_1	1.42(4)
C_{12}–N_{12}	1.55(3)	C_{22}–N_{22}	1.54(3)	C_2–N_2	1.60(4)

[a] See Table II.

On the other hand, the dihedral angle between the aromatic planes of *meso*-3-$PtCl_2$ amounts to 46°. Only the hydroxy group of the equatorially arranged aromatic ring is oriented toward the N–Pt–N plane with an O_2–N_2 distance of 2.813 Å and a dihedral angle N_2–C_2–C_{21}–C_{22} of 50°. The second phenolic hydroxy group is turned away from the chelate ring. For *meso*-3-$PtCl_2$, too, no O–H···O bonds are found in the solid state (O–O distance = 4.01 Å; see Table V).

IR Spectroscopy. To confirm the existence of the intramolecular hydrogen bridges the diastereomeric [1,2-bis(2-hydroxyphenyl)ethylenediamine]dichloroplatinum(II) complexes were investigated by infrared spectroscopy.

In order to assign the OH–, NH–, and Pt–Cl stretching vibrations of *meso*-3-$PtCl_2$ and (−)-3-$PtCl_2$, the IR spectra are compared with those of their related ligands *meso*-3 and (−)-3, the respective N-deuterated $PtCl_2$ complexes, and the sulfato derivatives *meso*-3-$PtSO_4$ and (−)-3-$PtSO_4$. The *meso*- and (−)-1,2-bis(2-hydroxyphenyl)ethylenediamines show for the NH_2 groups strong symmetric (ν_s) and antisymmetric (ν_{as}) stretching vibrations at 3360 cm^{-1} (ν_{as}), 3280 cm^{-1} (ν_s) (*meso*-3) and 3350 cm^{-1} (ν_{as}), 3300 cm^{-1} (ν_s) ((−)-3). The absorption bands of the OH groups, located in the region between 3700 and 2100 cm^{-1}, are markedly broadened due to strong hydrogen bridges.

The coordination to platinum(II) is accompanied by a change in number and location of the OH and NH frequencies. The symmetric and antisymmetric NH-stretching vibrations of *meso*-3-$PtCl_2$ are split up to five bands and even seven bands in the case of (−)-3-$PtCl_2$. The appearance of this high number of absorptions in the N–H region is well-known in the literature. For example, Berg et al.[13] interpret the four bands at 3275, 3250, 3200, and

(13) Berg, R. W.; Rasmussen, K. *Spectrochim. Acta* **1973**, *29A*, 319.

3117 cm^{-1} of the NH_2 groups of $enPtCl_2$ analogously to Watt et al.[14] by symmetric and asymmetric stretching vibrations and a Fermi resonance interaction with the $\delta(NH_2)$ deformation vibrations occurring at about 1590 cm^{-1} and an overtone of an NH_2 scissoring vibration. The bands of *meso*-**3**-$PtCl_2$ at 3275 cm^{-1} (ν_{as}), 3260 cm^{-1} (ν_{as}), 3200 cm^{-1} (ν_s), and 3120 cm^{-1} (ν_s) are assigned on the basis of these data.

The four NH-stretching vibrations in the spectrum of (–)-**3**-$PtCl_2$ are located at 3280 cm^{-1} (ν_{as}), 3260 cm^{-1} (ν_{as}), 3200 cm^{-1} (ν_s), and 3120 cm^{-1} (ν_s), with additional bands at 3235, 3230, and 3190 cm^{-1}. This assignment to N–H resonances has been confirmed by NH/ND isotope shifts in *meso*- and (–)-**3**-$PtCl_2$. The N–D wavenumbers are located between 2290 and 2440 cm^{-1}. Additionally, two bands with medium intensity at 2520, 2580 cm^{-1} for *meso*-**3**-$PtCl_2$ and 2520, 2555 cm^{-1} for (–)-**3**-$PtCl_2$ are found, assigned to O–D stretching vibrations. These phenolic O–D groups result from a partial OH/OD displacement during the NH/ND exchange. Furthermore, the NH_2 frequencies of *meso*- and (–)-**3**-$PtCl_2$ are lower than those of the free ethylenediamine ligands. Two reasons are held responsible for this shift. 1. Effect of coordination: Coordination of ethylenediamines results in strong Pt–N bonds and delocation of electrons from nitrogen to platinum(II). Therefore, the N–H bonds are weakened whereby the N–H frequencies are lowered.[15] 2. Formation of hydrogen bridges: Hydrogen bridges lengthen the N–H bond and lower the N–H stretching frequencies.

The lowering of hydrogen stretching frequencies by hydrogen bonds is well-known.[16,17] In the case of *meso*-**3**-$PtCl_2$ and (–)-**3**-$PtCl_2$ the X-ray analyses give evidence for inter- and intramolecular H-bonds originating from the N–H protons. *meso*-**3**-$PtCl_2$ shows in the solid state one, and (–)-**3**-$PtCl_2$, two N–H···O hydrogen bonds of different strength (different distances between O and N). The broad absorption band of chelatelike bonded OH groups in the spectra of the free ligands *meso*-**3** and (–)-**3** are replaced by one band at 3415 cm^{-1} for *meso*-**3**-$PtCl_2$ and two bands at 3400 and 3370 cm^{-1} for (–)-**3**-$PtCl_2$. These vibrations are due to isolated OH groups in the complexes. A comparable ν_{O-H} (3420 cm^{-1}) has been found by Appleton et al.[18] for [1,3-diaminopropan-2-ol]dichloroplatinum(II). This complex exists in a chair-type conformation of the chelate ring with an axially oriented hydroxy group,[19] stabilized by intramolecular H-bridges from the hydrogens of both amino groups to the hydroxy oxygen, with one ν_{N-H} band at 3275 cm^{-1} and three broad less resolved bands at lower frequencies.

The Pt–Cl stretching vibrations of *meso*- and (–)-**3**-$PtCl_2$ are assigned by comparison of the spectra with those of the sulfatoplatinum(II) complexes. Since the Pt–Cl stretching frequencies are a measure for the bond strength which determines the reactivity of dichloroplatinum(II) complexes, an exact assessment was carried out using an FT-IR spectrometer. Figure 5 presents the spectra of (–)-**3**-$PtCl_2$ and *meso*-**3**-$PtCl_2$. Both complexes show in the region of the Pt–Cl bands the same stretching vibrations. By comparison of these data with those of $enPtCl_2$,[13] the bands at 274, 308, and 326 cm^{-1} are ascribed to the Pt–Cl stretching vibrations. On the basis of identical stretching vibrations the same Pt–Cl bonding strength can be assumed for (–)-**3**-$PtCl_2$ and *meso*-**3**-$PtCl_2$.

^{1}H-NMR Spectroscopy. To investigate the structure of the [1,2-bis(2-hydroxyphenyl)ethylenediamine]platinum(II) complexes (–)-**3**-$PtCl_2$ and *meso*-**3**-$PtCl_2$ in solution ^{1}H-NMR spectroscopy was used. The ^{1}H-NMR spectra of *meso*-**3**-$PtCl_2$ and (–)-**3**-$PtCl_2$ are shown in Figures 6A and 7A.

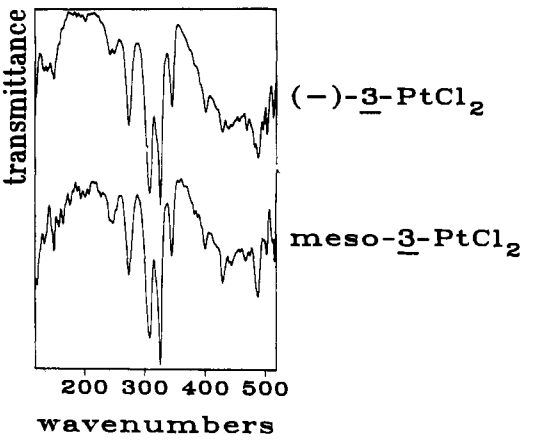

Figure 5. IR spectra of (–)-**3**-$PtCl_2$ and *meso*-**3**-$PtCl_2$.

To assign the benzylic and amino protons in the spectra D_2O is added to the complex solution (DMF-d_7). After NH/ND exchange the benzylic protons can be assigned to the signals at δ = 4.83 (*meso*-**3**-$PtCl_2$) and δ = 4.70 ((–)-**3**-$PtCl_2$). Thus the NH resonances are located at δ = 5.25 and 6.12 (*meso*-**3**-$PtCl_2$) and δ = 5.27 and 6.10 ((–)-**3**-$PtCl_2$). The NH signals as well as the $CH_{benzylic}$ signals are broadened by the coupling between NH, $CH_{benzylic}$, and ^{195}Pt. The presence of two NH resonances is a consequence of the five-membered chelate rings. Coordination to platinum blocks the rotation around the N–C axis and the N–H protons become diastereotopic, resulting in different signal groups for the protons arranged below and above the N–Pt–N plane.

The five-membered chelate ring is not flat but puckered with two energetically preferred conformations, the δ- and the λ-conformations, which should exist in equilibrium (interconversion of the five-membered chelate ring). Information whether this is true for *meso*-**3**-$PtCl_2$ and (–)-**3**-$PtCl_2$ is obtained from the related unsymmetric $Pt(SO_4)(DMSO\text{-}d_6)$ derivatives. These compounds are formed from the diastereomeric aqua[1,2-bis(2-hydroxyphenyl)ethylenediamine]sulfatoplatinum(II) complexes *meso*-**3**-$PtSO_4$ and (–)-**3**-$PtSO_4$ after dissolution in DMSO-d_6. Due to the unsymmetric $Pt(SO_4)(DMSO\text{-}d_6)$ moiety the NH as well as the $CH_{benzylic}$ protons are additionally diastereomerically split. Beside two CH signals four NH signals arise, which are partially superimposed by Ar H (see Figure 8A,C).

The spectra of the sulfatoplatinum(II) complexes can easily be simplified by exchanging the N-standing protons by deuterium, which affords an insight into the complex conformation. The spectrum of (–)-**3**-$PtSO_4$ (Figure 8D) shows (after NH/ND exchange) an AB pattern with a coupling constant of 12.4 Hz for the nonequivalent benzylic protons, indicating a dihedral angle between the protons of about 180°. This means that (–)-**3**-$PtSO_4$ exists predominantly in a conformation with bis-equatorially arranged aromatic rings.

On the other hand, in both the δ- and the λ-conformations of *meso*-**3**-$PtSO_4$ the rings are synclinally arranged. A fast interconversion between these conformers would entail one AB pattern with a median coupling constant of about 6.9 Hz, a slow δ–λ interconversion, and an AB pattern of about J_{H-H} = 5.2 Hz.[20] The coupling constant of J_{H-H} = 5.4 Hz found for *meso*-**3**-$PtSO_4$ (Figure 8B) is in good agreement with a slow or not existent interconversion of the five-membered chelate ring on the NMR time scale.

The hindrance of the chelate ring interconversion of [*meso*-1,2-bis(2-hydroxyphenyl)ethylenediamine]platinum(II) complex-

(14) Watt, G. W.; Hutchinson, B. B.; Klett, D. S. *J. Am. Chem. Soc.* **1967**, *89*, 2007.
(15) Nakamoto, K. *Infrared and Raman Spectra of Inorganic and Coordination Compounds*; Wiley: New York, 1978; p 197.
(16) Badger, R. M. *J. Chem. Phys.* **1940**, *11*, 288.
(17) Nakamoto, K.; Margoshes, M.; Rundle, R. E. *J. Chem. Soc.* **1955**, *77*, 6480.
(18) Appleton, T.; Hall, J. R. *Inorg. Chem.* **1972**, *11*, 117.
(19) Oksanen, A.; Kivekäs, R.; Lumme, P.; Laitalainen, T. *Acta Crystallogr. C47*, 719.
(20) Gust, R.; Burgemeister, Th.; Mannschreck, A.; Schönenberger, H. *J. Med. Chem.* **1990**, *33*, 2535.

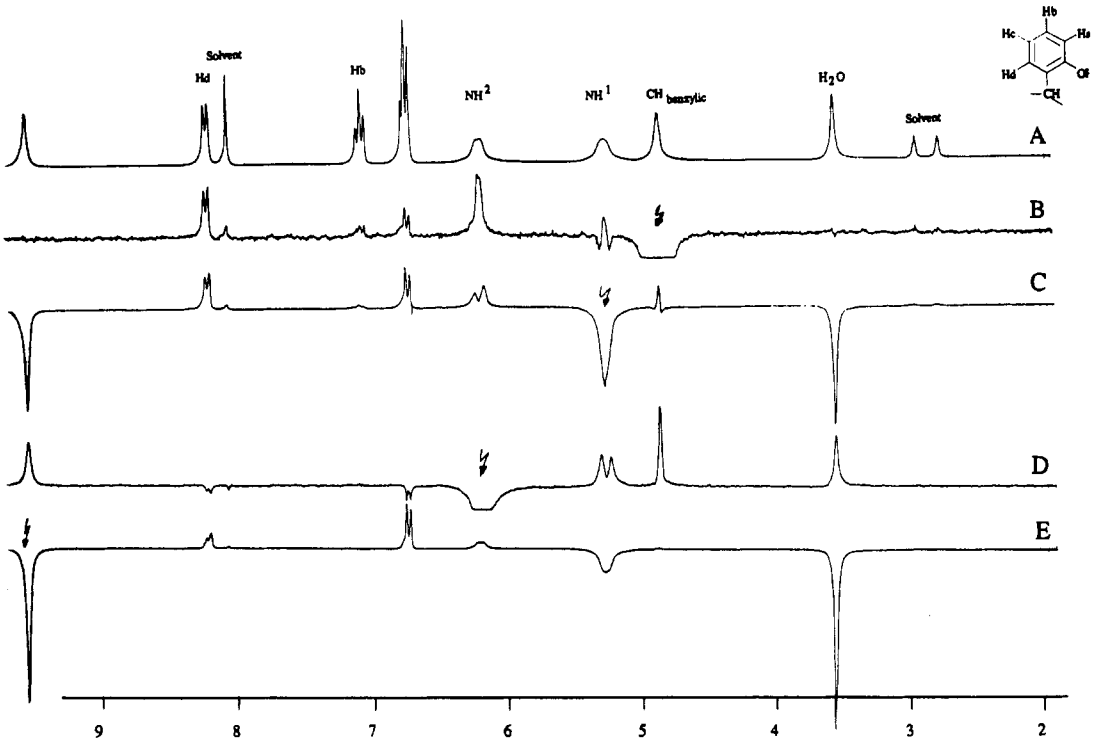

Figure 6. 250-MHz ^{1}H-NMR spectra of *meso*-3-$PtCl_2$ (A) in DMF-d_7 and 250-MHz ^{1}H NOE difference spectra due to the irradiation of $CH_{benzylic}$ (B), NH^1 (C), NH^2 (D), and OH (E) in *meso*-3-$PtCl_2$.

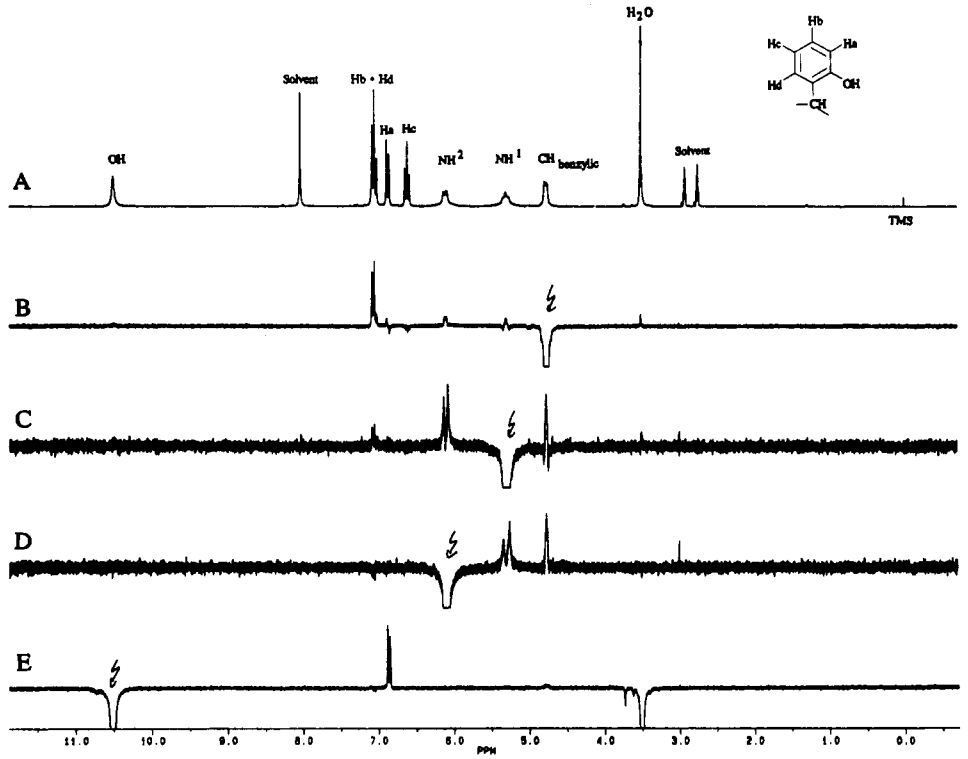

Figure 7. 250-MHz ^{1}H-NMR spectra of (–)-3-$PtCl_2$ in DMF-d_7 (A) and 250-MHz ^{1}H NOE difference spectra due to the irradiation of $CH_{benzylic}$ (B), NH^1 (C), NH^2 (D), and OH (E) in (–)-3-$PtCl_2$.

es can be ascribed to intramolecular hydrogen bonds. Such an effect is already known for the [1,3-diaminopropan-2-ol]dichloroplatinum(II) complex. Intramolecular H-bridges, proceeding from the amino protons to the OH oxygen stabilize the ligand in a chair-type conformation.[21]

For *meso*-3-$PtCl_2$ and (–)-3-$PtCl_2$, too, hydrogen bonds from the amino protons to the phenolic oxygen can be predicted from the X-ray diffraction. Prerequisites for this are nonrotating phenyl rings, permitting a defined arrangement of the OH groups to the amino protons.

An appropriate experiment to determine the arrangement of the phenolic OH groups is the nuclear Overhauser enhancement experiment (NOE).[22] In this double resonance experiment a

(21) Appleton, T.; Hall, J. R. *Inorg. Chem.* **1972**, *11*, 117.

(22) Neuhaus, D.; Williamson, T. *The Nuclear Overhauser Effect in Structure and Conformeric Analysis*; VCH: New York, 1989.

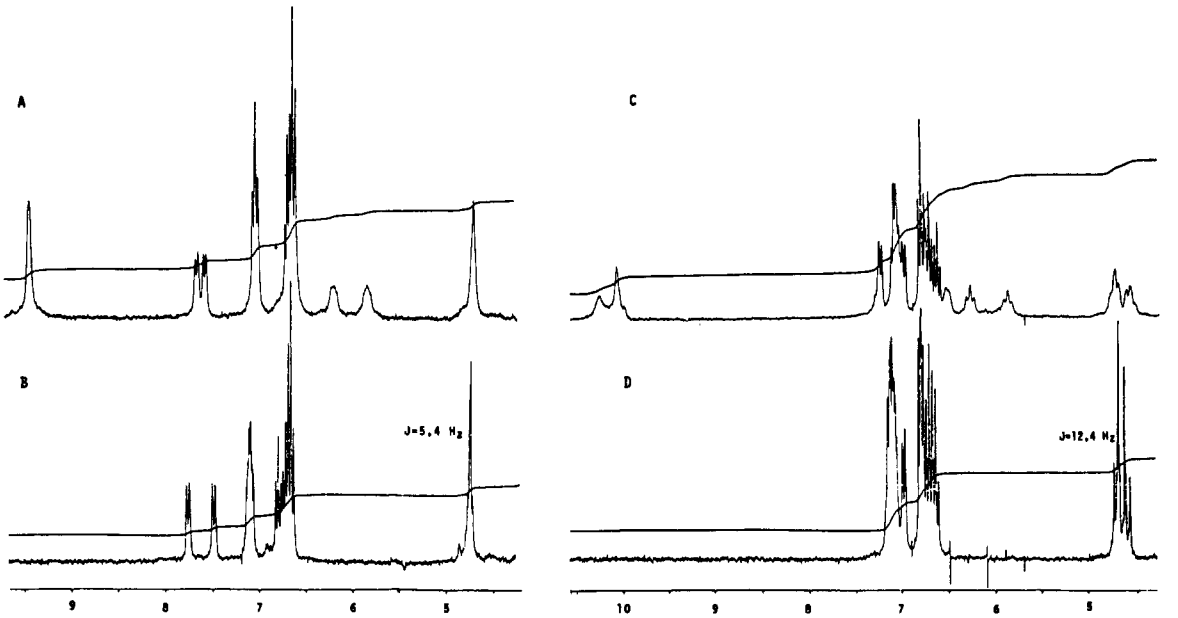

Figure 8. 250-MHz ^{1}H-NMR spectra of *meso*-3-$PtSO_4$ and (–)-3-$PtSO_4$: (A) *meso*-3-$PtSO_4$ in DMSO-d_6 (B) *meso*-3-$PtSO_4$ in DMSO-d_6 after N-deuteration; (C) (–)-3-$PtSO_4$ in DMSO-d_6; (D) (–)-3-$PtSO_4$ in DMSO-d_6 after N-deuteration.

saturation transfer is achieved between protons which are closer to each other than 3.5 Å. On the basis of distances found in the X-ray analysis of *meso*-3-$PtCl_2$ and (–)-3-$PtCl_2$, irradiation at the benzylic, amino, and phenolic protons should give an insight into the arrangement of the phenolic to the amino groups.

The ^{1}H-NMR spectrum of *meso*-3-$PtCl_2$ in deuterated dimethylformamide (see Figure 6A) contains beside $CH_{benzylic}$ and NH signals (see above) aromatic protons at 6.68–6.73 ppm (H^a + H^c), 7.01–7.08 ppm (H^b), and 8.16–8.19 ppm (H^d). The phenolic protons give a broad signal at 9.52 ppm. It is worthwhile to mention that solvent water appears at 3.56 ppm.

Saturation of the benzylic protons (Figure 6B) results in a strong intensification of the NH^2 signal and the aromatic H^d signal. The NOE $[CH_{benzylic}]NH^1$ is of small extent, so NH^2 can be assigned to both N,N′-standing amine protons located under the platinum plane, since they are closer to $CH_{benzylic}$. The NOE $[CH_{benzylic}]H^d$ and the simultaneously missing effect on the phenolic hydrogens indicate a restricted rotation of both phenyl rings, with an OH orientation to the NH^1 protons.

This is confirmed by irradiation at NH^2 (Figure 6D), whereby the $CH_{benzylic}$ and the NH^1 signals are intensified and NOEs of the phenolic OHs and the solvent water are found. On the other hand, NOEs of the NH^2 protons and negative signals at the phenolic hydrogens and the solvent water appear after saturation of the above the N–Pt–N plane standing NH^1 protons (Figure 6C). The latter effects result from saturation transfers between exchanging protons.

Irradiation at the OH signal (Figure 6E) confirms the observations discussed above. The NH^2 signal is intensified, while NH^1 and H_2O show the postulated proton exchange. This experiment leads, especially for Ar H^a, to an amplification; hence, this proton is assigned to the position neighboring the hydroxy group and Ar H^d to the ortho position. The resonance of the latter is strongly shifted to lower field due to the anisotropic effect of both phenyl rings.

Intramolecular NH exchanges were already found by Erickson et al. in $(NH_3)_3Pt–NH(CH_3)CH_2CO_2]^+$ under participation of the acetate fragment.[23] In the case of *meso*-3-$PtCl_2$ only the hydroxy groups can catalyze this reaction. However, it is impossible to decide whether the hydroxy group of the axially or of the equatorially arranged ring causes this effect.

Table VI. Chemical Shift of Benzylic and Amino Protons of *meso*- and *R,R/S,S*-Configurated 2-Substituted Dichloro[1,2-diphenylethylenediamine]platinum(II) Complexes in the ^{1}H-NMR Spectra[a]

	meso-complexes		*R,R/S,S*-complexes	
	2-H	2-OH	2-H	2-OH
–CH–	4.55	4.83	4.50	4.71
$–NH^1$	5.60	5.25	5.83	5.27
$–NH^2$	6.20	6.12	6.34	6.10

[a] The spectra were taken at 250 MHz in DMF-d_7 with TMS as an internal standard.

In contrast to this, the NOEs $[CH_{benzylic}]NH^1$ and $[CH_{benzylic}]$-NH^2 of (–)-3-$PtCl_2$ are of comparable strength (Figure 7B), because at any time one $CH_{benzylic}$ is in vicinity to NH^1 or NH^2. Irradiation at NH^1 and NH^2 confirms these H–H interactions (Figure 7C,D). The NOE $[CH_{benzylic}]H^d$ and the missing $[CH_{benzylic}]$OH NOE for (–)-3-$PtCl_2$ also point to a restricted rotation of the aromatic rings due to the NH···O bonds. Saturation of the NH protons has no effect on the OH or the solvent water. However, irradiation at the OH signal (Figure 7E) shows that OH protons and protons of the solvent water exchange, but the amino protons do not. The differences in the exchanging effects of *meso*- and (–)-3-$PtCl_2$ can be ascribed to different arrangements of the hydroxy groups in relation to the amino protons. In *meso*-3-$PtCl_2$ the phenolic oxygens are only involved in the hydrogen bonds to NH^1. By this the NH^1 protons are shifted to higher field. By the comparison with the amino signals of the ring-unsubstituted dichloro[*meso*-1,2-diphenylethylenediamine]platinum(II) complex (see Table VI), which exists in a flexible structure[24] (chelate ring interconversion and free rotation of the aromatic rings), an NH^1 shift of about 0.35 ppm is found, while the NH^2 resonance is only marginally influenced (ΔNH^2 = 0.08 ppm).

On the other hand, both protons are strongly shifted to high field (ΔNH^1 = 0.56 ppm, ΔNH^1 = 0.24 ppm; see Table VI) in the spectrum of (–)-3-$PtCl_2$. Therefore a structure can be assumed with both hydroxy groups located laterally to the N–Pt–N plane and with hydrogen bonds between these and both N,N-standing protons. The proposed structures of (–)-3-$PtCl_2$ and *meso*-3-$PtCl_2$ are presented in Figures 9 and 10.

(23) Erickson, L. E.; Fritz, H. L.; May, R. J.; Wright, D. A. *J. Am. Chem. Soc.* **1969**, *91*, 2513.

(24) Yano, S.; Tukada, T.; Saburi, M.; Yoshikawa, S. *Inorg. Chem.* **1978**, *17*, 2520.

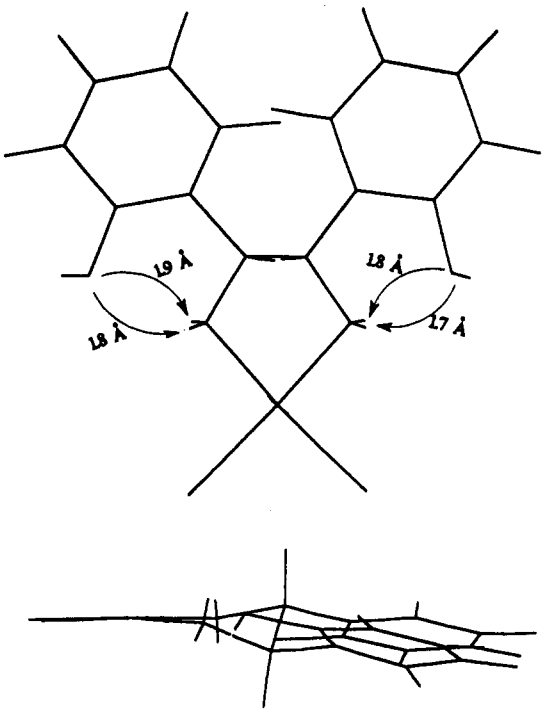

Figure 9. Structure of (–)-**3**-$PtCl_2$ in solution. Representation and measurement of NH···O distances were performed by use of the molecular modeling software Alchemy III.

For (–)-**3**-$PtCl_2$ the N–H···O distances from NH^1 and NH^2 to the hydroxy oxygen amount to about 1.7–1.9 Å (see Figure 9). In *meso*-**3**-$PtCl_2$ the N–H^1···O distances (1.4 Å/1.7 Å) are much smaller than the N–H^2···O ones (2.8 Å/3.0 Å) (see Figure 10). By comparison of these data, catalysis of exchanging effects on the N–H protons by hydroxy groups seems to take place only by an N–H···O approach close to 1.4 Å. In this case the N–H bonds are polarized and extended, whereby exchange reactions can occur.

The structures of *meso*-**3**-$PtCl_2$ and (–)-**3**-$PtCl_2$ in solution are different from those in the solid state. After dissolution in DMF-d_7, the hydroxy group of the axially arranged ring in *meso*-**3**-$PtCl_2$ is orientated to the central platinum atom by rotation around the benzylic axis. The OH groups of the equatorially arranged rings are reoriented as well. In the solid state they are arranged directly above the platinum plane, while in solution the hydrogen bonds displace them laterally to it. By this and due to the missing rotation of the aromatic rings (–)-**3**-$PtCl_2$ exists as a very plain molecule (see Figure 9). *meso*-**3**-$PtCl_2$ possesses a conformation with groups accumulated above the N–Pt–N plane (one aromatic ring is axially arranged; see Figure 10).

These steric differences are of great importance for substitution reactions on *meso*-**3**-$PtCl_2$ and (–)-**3**-$PtCl_2$. Nucleophilic attacks at the platinum of *meso*-**3**-$PtCl_2$ are rendered more difficult compared to (–)-**3**-$PtCl_2$.

Solution Chemistry. In order to study the influence of the 1,2-diphenylethylenediamine ligand on the reactivity of the complexes, *meso*-**3**-$PtCl_2$ and (–)-**3**-$PtCl_2$ were reacted in aqueous solution with I^-. To monitor the formation rates of the reaction products, an HPLC system with UV detection was used. I^- was given the priority to other nucleophilic agents, since the resulting chloroiodo- and diiodoplatinum(II) complexes eluate quantitatively from the RP-18 HPLC column with excellent separation. Furthermore I^- coordinates to platinum in a stabile Pt–I bond, so no reaction step is reversible.

According to Scheme I the substitution of Cl^- leaving groups by I^- can happen in two different pathways. The first pathway is called the solvent path, by which a H_2O molecule substitutes a Cl^- in a slow step building the monoaquaplatinum(II) species (hydrolysis, rate constants = $k_{1,s}$,$k_{2,s}$). In a fast reaction the

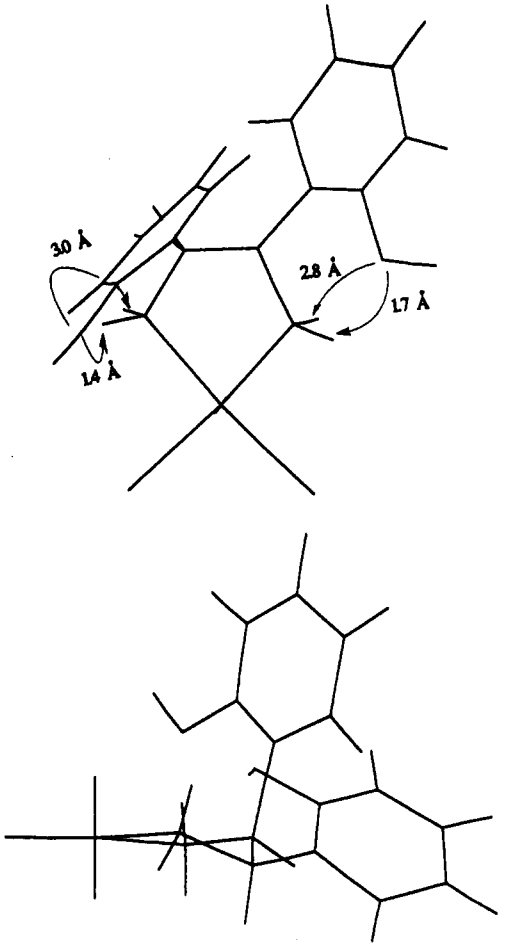

Figure 10. Structure of *meso*-**3**-$PtCl_2$ in solution. Representation and measurement of NH···O distances were performed by use of the molecular modeling software Alchemy III.

water molecule is substituted by I^- ($k_3 \gg k_{1,s}$, $k_5 \gg k_{2,s}$). Parallel to this, a direct attack of I^- can occur (rate constants = k_{1,I^-},k_{2,I^-}) in a second nucleophilic pathway.

The rate law governing substitution in planar platinum complexes usually consists of two terms, one first order in the metal complex and the other first order in both complex and the entering I^-:

$$V = k_s[\text{complex}] + k_{I^-}[\text{complex}][I^-]$$

If I^- is used in excess, the reaction follows pseudo-first-order dependence. The experimental first-order rate constant k_{obs} is given by

$$V = k_{obs}[\text{complex}]$$

Therefore

$$k_{obs} = k_s + k_{I^-}[I^-]$$

Evaluation of reaction curves of 50 μM solutions of the complexes *meso*-**3**-$PtCl_2$ and (–)-**3**-$PtCl_2$ with increasing amounts of KI (10-, 100-, 500-, 1000-fold excess) yields $k_{1,obs}$ and $k_{2,obs}$, dependent on the concentration of the entering nucleophile I^-.

In accordance with the proposed two-path mechanism, the exchange of the Cl^- leaving groups gives plots $k_{1,obs}$ vs $[I^-]$ and $k_{2,obs}$ vs $[I^-]$, which have linear correlations with intercepts $k_{1,s}$ and $k_{2,s}$ and slopes k_{1,I^-} and k_{2,I^-} of the straight lines.

In Figure 11 the correlations for *meso*-**3**-$PtCl_2$ and (–)-**3**-$PtCl_2$ are shown. For both reaction steps a clear dependence of the reaction rate on the I^- concentration with very good linear correlation factors > 0.99 are found. So the substitution reaction on [1,2-bis(2-hydroxyphenyl)ethylenediamine]platinum(II) com-

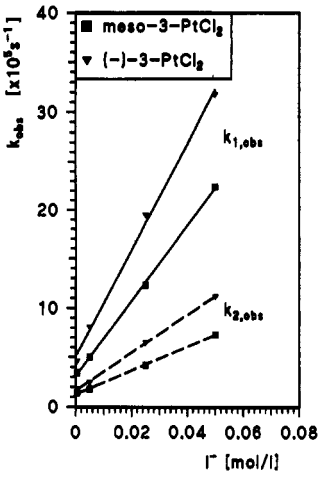

Figure 11. Rate of reactions of *meso*-3-$PtCl_2$ and (-)-3-$PtCl_2$ in water at 26 °C as a function of different KI concentrations.

Scheme I

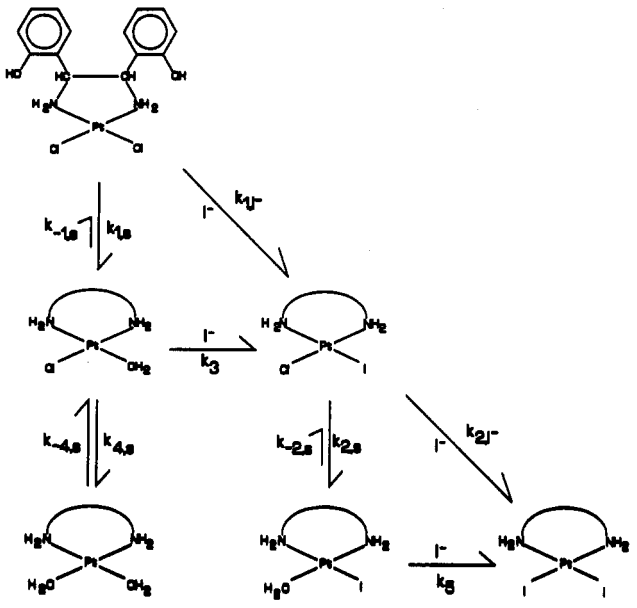

plexes follows the two-path mechanism, via hydrolysis and direct nucleophilic attack. $K_{1,s}$, $k_{2,s}$, k_{1,I^-}, and k_{2,I^-} values are listed together with the $k_{1,obs}$ and $k_{2,obs}$ values in Table VII.

It is of interest to note that the reaction rates were found to be independent of the ionic strength. Therefore the reactions were performed without constant ionic strength. During the substitution reactions the pH values of the solutions did not change and amounted to pH = 5.8–6.2.

Since hydrolysis is of importance for the reaction of dichloroplatinum(II) complexes with DNA, the first Pt–Cl hydrolysis rates of *meso*-3-$PtCl_2$ and (-)-3-$PtCl_2$ were determined in a second experiment to confirm the accuracy of the used reaction system. For this purpose the time-dependent change of the hydrolysis products of a 50 μM aqueous solution of the complexes was determined. Due to the high reactivity of the resulting monoaqua- and diaquaplatinum(II) complexes they eluate incompletely from the end-capped, RP-18 column owing to irreversible reactions with residual silanol groups of the RP-18 stationary phase. So is is necessary to trap the products with I^-, by conversion into the neutral, low reactive chloroiodo- and diiodoplatinum(II) complexes, which eluate quantitatively relative to the injected dichloroplatinum(II) complex. Under the conditions of KI addition (25 mM, 2 min) a complete exchange of the coordinated water takes place. Higher concentrations of KI and a longer reaction time (>2 min) lead to a direct exchange of Cl^- by I^-.

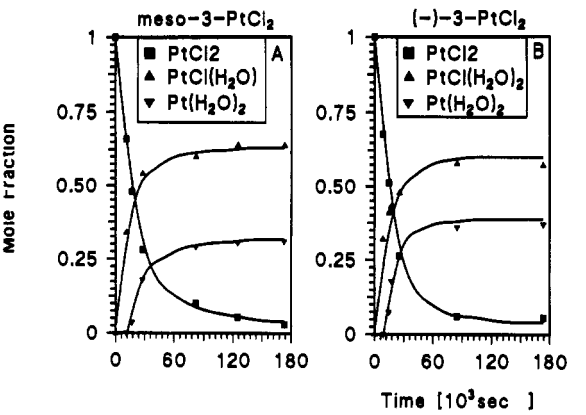

Figure 12. Time-dependent concentrations of hydrolysis products of *meso*-3-$PtCl_2$ (A) and (-)-3-$PtCl_2$ (B) trapped with 25 mM KI.

Table VII. Reaction Rate Constants of the Dichloroplatinum(II) Complexes *meso*-3-$PtCl_2$ and (-)-3-$PtCl_2$

			rate const × 10^5, s^{-1}	
compd	KI concn, mM	T, °C	$k_{1,obs}$	$k_{2,obs}$
meso-3-$PtCl_2$	0.0	26	3.3 ● 0.5	n.d.
	0.5	26	3.4 ± 0.2	1.4 ± 0.3
	5.0	26	5.0 ± 0.3	1.8 ± 0.4
	25.0	26	12.3 ± 0.7	4.2 ± 0.5
	50.0	26	22.4 ± 1.6	7.3 ± 1.0
(-)-3-$PtCl_2$	0.0	26	4.7 ± 2.0	n.d.
	0.5	26	4.6 ± 0.5	1.8 ± 0.3
	5.0	26	8.1 ± 0.6	2.5 ± 0.4
	25.0	26	19.5 ± 0.8	6.5 ± 0.5
	50.0	26	31.8 ± 1.6	11.2 ● 0.9

	rate const			
compd	10^5 $k_{1,s}$, s^{-1}	k_{1,I^-}, L/mol·s	10^5 $k_{2,s}$, s^{-1}	k_{2,I^-}, L/mol·s
meso-3-$PtCl_2$	3.06	383.5	1.26	120.2
(-)-3-$PtCl_2$	5.05	543.9	1.64	191.6

Figure 12 shows the time-dependent concentration of hydrolysis products of *meso*-3-$PtCl_2$ (A) and (-)-3-$PtCl_2$ (B).

The hydrolysis follows two consecutive pseudo-first-order reactions according to Scheme I but under participation of reversible substitution steps. While the dichloroplatinum(II) complexes hydrolyze nearly quantitatively, the monoaqua and diaqua species exist in an equilibrium at the end of the reaction. For the first hydrolysis step a participation of a reversible reaction is found, too, but an estimation for the first rate constant (k_1) is possible from the slope of the semilog plot of the $PtCl_2$ decrease vs time at the beginning of the hydrolysis. Comparison with the data given from the reaction with I^- indicates a very good reproducibility of this method (see Table VII).

The results listed in Table VII show that the Cl^- hydrolysis of all complexes is delayed compared to cisplatin ($k_{1,s} = 6.32 \times 10^{-5}$ s^{-1} and $k_{2,s} = 2.50 \times 10^{-5}$ s^{-1}).[25] This seems to be the consequence of a steric hindrance during the attack of the entering ligand. Steric factors may markedly slow substitution rates of planar four-coordinated d^8 metal complexes, in agreement with a process involving expansion of the coordination sphere.[26] Substitution reactions on complexes are generally classified as having either dissociative or associative mechanisms. Platinum complexes like the diastereomeric [1,2-bis(2-hydroxyphenyl)ethylenediamine]-dichloroplatinum(II) complexes, in which the coordination number is less than 6, would be more likely to react by an associative process. In a first slow step the entering nucleophile is associated with the platinum to form an intermediate with a coordination number of 5, arranged as a trigonal bipyramid.

(25) Reishus, J. W.; Martin, D. S., Jr. *J. Am. Chem. Soc.* **1961**, *83*, 2457.
(26) Belluco, U. In *Organometallic and Coordination Chemistry of Platinum*; Maitlis, P. M., Stone, F. G. A., West, R., Eds.; Academic Press: London and New York, 1974; p 138.

Scheme II

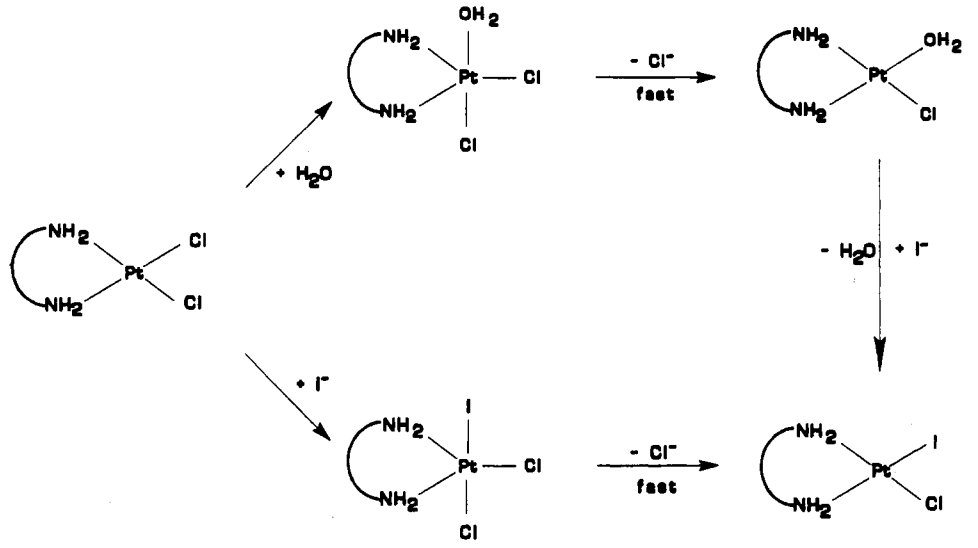

Table VIII. Antitumor Effects of *R,S*-, *R,R*-, and *S,S*-Configurated [1,2-bis(2-hydroxyphenyl)ethylenediamine]dichloroplatinum(II) Complexes on the P388 Leukemia of the CD_2F_1 Mouse

compd	day of injection	single dose[a] μmol/kg	single dose[a] mg/kg	animal body weight change days 1–5	median survival time days	median survival time range in days	T/C, %	animals survived
control	1–9			–0.4	9	8–11	100	0/10
cisplatin[b]	1–6	3.3	1.0	3.4	20	9–30	200	3/10
meso-3-$PtCl_2$[b]	1–9	6.6	3.37	0.4	14	10–14	140	06
	1–9	3.3	1.68	1.5	12.5	12–19	125	0/6
(+)-3-$PtCl_2$	1–5	10.2	5.05	4.1	21.5	9–33	239	0/6
	1–5	6.6	3.37	3.8	22.5	7–24	250	0/6
	1–9	3.3	1.68	2.6	19	17–20	211	0/6
(–)-3-$PtCl_2$	1–5	10.2	5.05	4.8	7	7–8	88	0/6
	1–5	6.6	3.37	5.2	30	30	300	5/5
	1–9	3.3	1.68	2.5	25.5	22–30	283	1/6

[a] The compounds were administered intraperitoneally as a polyethylene glycol 400/1.8% NaCl solution. [b] Data from ref 10.

Subsequent loss of a chloride leaving group is fast, giving again the square planar platinum complex (compare Scheme II). Most reactions proceed with both bond breaking and bond making simultaneously, so detection of an intermediate is impossible in most cases.

Cisplatin is a square planar complex with NH_3 ligands of small size. Thus, association of nucleophiles is easily possible. Such a complex will be attached to highly reactive substrates. In the case of the [1,2-bis(2-hydroxyphenyl)ethylenediamine]dichloroplatinum(II) complexes, the ethylenediamine ligands delay the nucleophilic attack.

(–)-3-$PtCl_2$ exists in solution in a conformation with bis-equatorially arranged aromatic rings. An interconversion of the five-membered chelate ring and therefore a reorientation of the phenyl rings into an axial position is not observed. Additionally the rings are fixed due to NH···O hydrogen bonds. Consequently the complexes are nearly flat (see Figure 9), so the nucleophilic attack perpendicular to the platinum plane is only slightly hindered compared to cisplatin.

On the other hand, *meso*-3-$PtCl_2$ possesses in aqueous solution a conformation of the ethylenediamine ligand with an axially arranged aromatic ring. In the most stable conformation of *meso*-3-$PtCl_2$ the oxygen of the axially-standing 2-hydroxyphenyl residue is close to the central platinum(II) atom.[27] Molecular mechanics calculations (MM2) confirm the discussed conformations of the diastereomers and show that *meso*-3-$PtCl_2$ possesses a 6.7 kJ mol^{-1} higher energy than (–)-3-$PtCl_2$. Since at room temperature no interconversion of the five-membered chelate ring takes place in *meso*-3-$PtCl_2$, the association of the entering nucleophile is rendered more difficult. Therefore *meso*-3-$PtCl_2$ is markedly less reactive than its diastereomer.

The results obtained from the experiments indicate furthermore that mainly steric effects of the 1,2-diphenylethylenediamine ligands determine the reaction rates. Electronic effects are of only subordinate importance for substitution reactions.

The increased electron density compared to that of cisplatin, resulting from N–H···O hydrogen bonds, should strengthen the Pt–N bond and thereby activate the trans-position via the higher trans effect for a nucleophilic exchange. Unequally strong H-bonds as found in *meso*-3-$PtCl_2$ should influence the rate constants for both reaction steps in different ways, changing the $k_{1,s}/k_{2,s}$ ratio. In fact, the same $k_{1,s}/k_{2,s}$ proportions for *meso*-3-$PtCl_2$ (2.43) and cisplatin (2.53) were found. Since in this respect (–)-3-$PtCl_2$ (3.08), too, deviates only marginally from cisplatin; the decreased reactivity of the diastereomeric [1,2-bis(2-hydroxyphenyl)ethylenediamine]dichloroplatinum(II) complexes in comparison to cisplatin results only from steric effects.

Reactivity of the Platinum Complexes in Relation to Their Antitumor Activity. For the correlation of the reaction rates with *in vivo* antitumor effects, the results on the murine lymphocytic leukemia P388, which is highly sensitive against platinum complexes, are used. The effects of *meso*-3-$PtCl_2$, (–)-3-$PtCl_2$, and also (+)-3-$PtCl_2$ are listed in Table VIII. Cisplatin is used as reference. Among the tested complexes *meso*-3-$PtCl_2$ possessed the lowest activity. The highest used dose of 6.6 μmol/kg administered on days 1–9 led only to marginal antitumor effects (T/C = 140%), with no detectable toxic side effects.

In contrast to this the animals treated with (+)-3-$PtCl_2$ and (–)-3-$PtCl_2$ showed already at a dose of 3.3 μmol/kg reduced body weights. Higher doses limited the administration to days

(27) Nikolov, G. St.; Trendafilova, N.; Schönenberger, H.; Gust, R.; Kritzenberger, J.; Yersin, H. Manuscript in preparation.

1–5, due to the toxic side effects. Nevertheless, all doses used led to strong tumor-inhibiting effects. While (+)-3-$PtCl_2$ showed a T/C = 250% at a 6.6 μmol/kg dose, (–)-3-$PtCl_2$ reached a maximal T/C value of 300%, whereby all animals were free of tumors.

Furthermore, (–)-3-$PtCl_2$ surpassed the effects of cisplatin. In the 3.3 μmol/kg dose (which is the highest tolerable for cisplatin) the T/C value amounted to 283% with one tumor-free animal out of six at the end of the test. Compared to this, cisplatin showed only a T/C value of 200%, with 3 out of 10 surviving animals. At this dosage (+)-3-$PtCl_2$ (T/C = 211%) was equiactive to cisplatin (T/C = 200%), however, without surviving animals. Consequently, the *in vivo* activity of the complexes increased in the order

meso-3-$PtCl_2$ < (+)-3-$PtCl_2$ < cisplatin < (–)-3-$PtCl_2$

The reactivity of the complexes determines both the antitumor activity and the toxicity. The latter results from the binding of the drugs to bionucleophiles during the transport of platinum complexes through the body.

For cisplatin, the nucleophilic agents which cause reactions are found to be water and especially sulfur-containing bionucleophiles. Concerning the rate-determining step of the substitution of sulfur-containing bionucleophiles on platinum, the available data are rather controversal. It has been suggested that cysteine,[28,29] glutathione,[28,29] metallothionein,[30] and adenosine triphosphatase[31] bind directly via a nucleophilic attack to cisplatin. However, the hydrolysis is reported to be the rate-determining step in the reaction of cisplatin with aminopeptidase,[31] γ-glutamyl transpeptidase,[31,32] and albumin.[33]

Due to their reduced reactivity, the [1,2-bis(2-hydroxyphenyl)-ethylenediamine]platinum(II) complexes should yield higher drug levels and therefore have a stronger tendency to accumulate in tumor cells than cisplatin does.

On the other hand, high reactivity is of importance for the binding to DNA after accumulation in the tumor cells. For coordination to nucleobases of the DNA, the drugs have to hydrolyze in a rate-determining step in a first fast reaction.

The binding to DNA occurs, and in a second reaction step the platinum complexes form intrastrand cross-links, which damage the DNA function by leading to an arrest in DNA synthesis. A delayed reaction in the second substitution step will lead to enhanced DNA repair and lower antitumor effects.

Though *meso*-3-$PtCl_2$ should afford a high drug level due to its low reactivity, its antitumor activity is only poor. Both the first and the second substitution step of a chloride leaving group are delayed. If this complex is accumulated in the cells, the reactions with DNA as well as the formation of intrastrand cross-links are supposed to be slow, so this drug can be removed by repair enzymes.

In comparison, (–)-3-$PtCl_2$ and (+)-3-$PtCl_2$ exhibit a medium reactivity, lower than that of cisplatin but higher than that of *meso*-3-$PtCl_2$. The bioavailability and the kinetics of DNA binding seem to be of ideal character. Therefore high antitumor activities are found. After translocation into the tumor cells (–)-3-$PtCl_2$ and (+)-3-$PtCl_2$ bind to nucleobases of the DNA (preferentially guanine) with the same kinetics, according to their equal hydrolysis. In this reaction step the enantiomeric complexes form diastereomeric products due to the binding to the chiral DNA, which are supposed to react at different rates in the following reaction with neighboring nucleobases under loop formation, inducing different antitumor effects.

The mechanism of action discussed above is supported by observations *in vitro* on the NIH:OVCAR-3 cell line.[34] On this cell line (–)-3-$PtCl_2$ and cisplatin produce antitumor effects (T/C_{corr} = 49% and 45% at 5 μM, respectively) after a drug–cell contact of 1 h, followed by an incubation during 243 h in drug-free medium. In the same experiment the T/C_{corr} was found to be 76% for (+)-3-$PtCl_2$, while *meso*-3-$PtCl_2$ was inactive.

Due to the fast second reaction step (bifunctional binding) of (–)-3-$PtCl_2$ and of cisplatin the arrest of the DNA synthesis seems to take place already at a short-time drug incubation. On the other hand, the probably longer existing monoadducts of (+)-3-$PtCl_2$ and especially of *meso*-3-$PtCl_2$ could be removed by repair enzymes. But incubation of the cells with (+)-3-$PtCl_2$ over a longer period finally leads to the same portion of intrastrand cross-linked complexes as found with (–)-3-$PtCl_2$, giving the same antitumor effects but with a delayed onset of activity with (+)-3-$PtCl_2$. Owing to lower reactivity, the effects of *meso*-3-$PtCl_2$ are reduced.

Conclusion

The relations found among spatial structure, reactivity with nucleophiles, and cytotoxic activity of the studied platinum(II) complexes suggest that (–)-3-$PtCl_2$ owes its—relative to *meso*-3-$PtCl_2$—markedly stronger antitumor effects to its specular spatial structure, which should permit a better approach to the target DNA, as well as to its favorable reaction rate, which is of relevance for the interaction with nucleophilic centers in the DNA. In this context the newly developed HPLC assay, allowing one to investigate the reactivity of platinum complexes in the presence of I^- as a nucleophile, has proved to be a useful tool for the assessment of novel platinum complexes with regard to their antitumor potency in question, their interaction rates due to the binding to bionucleophiles, and their toxic side effects. Binding kinetics of the complexes to DNA and other bionucleophiles will complement this study.

Experimental Section

Materials and Methods. Synthesis. The syntheses of the diastereomeric 1,2-bis(2-hydroxyphenyl)ethylenediamines *meso*-3 and (±)-3, the resolution into the enantiomers (–)-3 and (+)-3, and the transformation into the dichloro- and sulfatoplatinum(II) complexes (*meso*-3-$PtCl_2$, *meso*-3-$PtSO_4$, (+)-3-$PtCl_2$, (+)-3-$PtSO_4$, (–)-3-$PtCl_2$, (–)-3-$PtSO_4$) have been described in previous papers.[10,35]

X-ray Crystallography. Colorless crystals of the compounds *meso*-3-$PtCl_2$ and (–)-3-$PtCl_2$ were grown by slow evaporation of a methanol/water solution of the complexes at room temperature. The crystal structures were solved by direct methods. Full-matrix refinement of *F*-values was performed with the program SDP.[36] Experimental data for both compounds are listed in Table I.

IR Spectroscopy. IR spectra were recorded on KBr pellets with a Perkin-Elmer 580 spectrophotometer or on polyethylene pellets with a Nicolet Model-60 SX FT-IR spectrometer (resolution 4 cm^{-1}, 20 scans).

^{1}H-NMR Spectroscopy. The ^{1}H-NMR spectra were taken with a Bruker PFT-NMR WM 250 spectrometer at 250 MHz and at a temperature of 297 K. Dimethylformamide-d_7 for dichloroplatinum(II) complexes and dimethyl-d_6 sulfoxide for sulfatoplatinum(II) complexes were used as solvents with tetramethylsilane as an internal standard. The complex concentrations used were 5 mg/mL.

(28) Corden, B. J. *Inorg. Chim. Acta* **1987**, *137*, 125.
(29) Andrews, P. A.; Murphy, M. P.; Howell, S. B. *Mol. Pharmacol.* **1986**, *30*, 643.
(30) Otvos, J. D.; Petering, D. H.; Shaw, C. F. *Comments Inorg. Chem.* **1989**, *9*, 1.
(31) Dedon, P. C.; Borch, R. F. *Biochem. Pharmacol.* **1987**, *36*, 1955.
(32) Bodenner, D. L.; Dedon, P. C.; Keng, P. C.; Borch, R. F. *Cancer Res.* **1986**, *46*, 2745.
(33) LeRoy, A. F.; Thompson, W. C. *J. Natl. Cancer Inst.* **1989**, *81*, 427.
(34) Bernhardt, G.; Gust, R.; Reile, H.; vom Orde, H. D.; Müller, R.; Keller, Chr.; Spruss, Th.; Schönenberger, H.; Burgemeister, Th.; Mannschreck, A.; Range, K. J.; Klement, U. *J. Cancer Res. Clin. Oncol.* **1992**, *118*, 209.
(35) Bernhardt, G.; Gust, R.; Reile, H.; vom Orde, H. D.; Müller, R.; Keller, Chr.; Spruss, Th.; Schönenberger, H.; Burgemeister, Th.; Mannschreck, A.; Range, K. J.; Klement, U. *J. Cancer Res. Clin. Oncol.* **1992**, *118*, 201.
(36) Enraf-Nonius Structure Determination Package, Version 3.1, Enraf-Nonius, Delft, The Netherlands, 1988.

HPLC Analyses. The HPLC analyses were done with a Kontron high-pressure mixing gradient system (Kontron 430 HPLC pump), a Kontron HPLC autosampler, and a Kontron 430 HPLC UV detector. A 0.4 × 25 cm Nucleosil-100 RP 18 column (Macherey-Nagel, Düren, FRG) with a 0.4 × 3.0 cm precolumn was used for chromatography. Eluent flow rate was 0.7 mL/min. Water was deionized by means of a Millipore Milli Q Water System to a resistivity of 1.8 M Ω cm. Methanol, Baker Analyzed HPLC Reagent (Fa. Baker, Deventer, Holland), Na_2SO_4 (pa; Fa. Merck, Darmstadt, FRG), and KI Suprapur (Fa. Merck, Darmstadt, FRG) were used.

The starting and reaction products (*meso*- and (–)-3-PtX_2, X = Cl and I, respectively) are well detectable by UV spectroscopy. Due to the large extinction coefficients of the diastereomeric ligands at λ_{max} = 276 nm, the sensitivity of this HPLC method is very high. The change in the UV absorption associated with the exchange of Cl^- by I^- is comparatively small. At the wavelength λ_{max} = 276 nm the differences between *meso*-3-$PtCl_2$ (ϵ = 6600 cm^{-1} M^{-1}) and *meso*-3-PtI_2 (ϵ = 6609 cm^{-1} M^{-1}) as well as (–)-3-$PtCl_2$ (ϵ = 6040 cm^{-1} M^{-1}) and (–)-3-PtI_2 (ϵ = 6104 cm^{-1} M^{-1}) amount to ≤1%, so the HPLC data of the dihaloplatinum(II) complexes are used uncorrected to determine the kinetic rate constants. For the chloroiodoplatinum(II) derivatives a comparable UV absorption is assumed.

In each experiment at least 10 time points were measured. Integration of the peak area was done by use of the Kontron 450MT data system. The mole fractions c were calculated from the respective peak areas as fractions of the total peak area. The rate constants were calculated according to the kinetic schemes described in the text by methods of the formal reaction kinetics.[37]

Pt–Cl Hydrolysis Assay. The reaction rate constants of the complexes *meso*-3-$PtCl_2$ and (–)-3-$PtCl_2$ were determined in deionized water at 26 °C. All reactions were performed in silylanized 1.7-mL glass vials. Stock solutions of *meso*-3-$PtCl_2$ and (–)-3-$PtCl_2$ (2.5 × 10^{-3} M) in methanol were prepared immediately prior to use. The methanol solutions were diluted 50 times in deionized water to a final concentration of 50 μM platinum complex. Immediately after this, and then in intervals of 100 min, 70-μL aliquots were removed from the reaction mixture and reacted with 70 μL of a 25 mM KI solution for 2 min. A 70-μL volume of this KI-quenched solution was loaded onto the HPLC column and eluated. For *meso*-3-$PtCl_2$ an isocratic system of 70:30 methanol/20 mM Na_2SO_4, pH 3.0, was used. The same system was applied for (–)-3-$PtCl_2$, however, containing 60:40 methanol/20 mM Na_2SO_4, pH 3.0.

Reaction of the Dichloroplatinum(II) Complexes with KI. The experiments were carried out by mixing the 2.5 × 10^{-3} M methanolic complex solution with an aqueous 5 × 10^{-4}, 5 × 10^{-3}, or 5 × 10^{-2} M KI solution. The analysis of the product mixture was performed with HPLC as described above.

Biological Methods. P388 Leukemia of the CD_2F_1 Mouse. The P388 leukemia was kindly provided by Dr. A. E. Bogden, EG&G Bogden Laboratories, Worcester, MA. This tumor was maintained by routine passage in female DBA/2 mice (Ivanovas, Kissleg, FRG). For determination of the antitumor activity, female CD_2F_1 mice (18–22 g, Zentralinstitut für Versuchstierzucht, Hannover, FRG) were inoculated ip with 10^6 leukemia cells in 0.1 mL of PBS buffer (day 0). The animals were randomly assigned to groups of 6 (10 animals to the solvent control), and the compounds were administered ip in polyethylene glycol 400/1.8% aqueous NaCl solution 1:1 on days 1–9. Cisplatin served as a positive control. The antitumor activity was evaluated as median day of survival time compared to the untreated control.

Acknowledgment. This work was supported by the Deutsche Forschungsgemeinschaft (SFB 234) and the "Matthias-Lackas-Stiftung fü Krebsforschung". Thanks are due to the Fonds der Chemischen Industrie for financial support. The excellent technical assistance of L. Schneider, S. Paulus, and F. Kastner is gratefully acknowledged.

(37) Frost, A. A.; Pearson, A. R. G. *Kinetics and Mechanism*; John Wiley & Sons, Inc.: New York, 1961.